Crystal Structure and ESIPT Phenomena of Anionic 2*H*-Phenanthro[9,10-*c*]pyrazol-11-ols

LI Chen-Chen(李晨晨);HE Yun (贺云);WEI Tao(魏涛);WANG Tao(王涛);ZHANG Zun-Ting(张尊听)

School of Chemistry and Chemical Engineering, Shaanxi Normal University, Xi´an 710062, *China*

ABSTRACT Using 4´-methoxy-5-hydroxyisoflavone and 4´,5-dihydroxy-7-methoxyisoflavone as leding compounds, 6-methoxy-2*H*-phenanthro[9,10-*c*]pyrazol-11-ol (**1a**) and 9-methoxy-2*H*-phenanthro [9,10-*c*]pyrazol-6,11-diol (**1b**) were synthesized by two dehydration processes in the EtOH solution. They were characterized by IR, ^{1}H NMR and ^{13}C NMR. The black prism crystal of **1a** was grown by the slow solvent evaporation technique from 40:1 (v/v) $CHCl_3$/MeOH, and it was determined by single-crystal X-ray diffraction. In the crystal structure, **1a** was stabilized by intramolecular (O–H ··N) and intermolecular (N–H ··O, O–H ··O, π ··π, C–H ··π) interactions. In addition, the fluorescence properties of **1a** and **1b** in the base and neutral media revealed that they possessed excited state intramolecular proton transfer phenomena (ESIPT).

Keywords: isoflavone; photocyclization;crystal structure;fluorescence;ESIPT;
DOI: 10.14102/j.cnki.0254-5861.2011-1724

1 INTRODUCTION

Excited state intramolecular proton transfer (ESIPT) is a special excited state photophysical process, which was reported including derivatives of benzophenones, flavones, anthraquinones, quinolines, quinoxalines, benzazoles, azoles, and salicylidene anilines[1-4]. An interesting feature of this process is that the molecule usually exhibits tautomerism and leads to significant emission wavelength red-shift of the molecules[5, 6]. It also has been applied in a variety of areas like laser dyes, photostabilisers, radiation scintillators, luminescent materials, molecular probes, sensing ions, photo-switching of polymorphs and so forth[7-9].

Pyrazole and its derivatives play an important role in heterocycles because of their wide applications. They are found to exhibit important biological and pharmaceutical activities[10, 11], such as anti-inflammatory[12], antitumor[13], anticancer[14], analgesic[15] and anti-fertility activities[16]. In addition,

heterocyclic aromatic compounds (HACs) of pyrazole ring as matrix are paid attention to because of their unique properties and potential applications due to their special structures[17, 18]. Based on our previous work[19], in this paper, a hydroxyl group was introduced to the skeleton of 2*H*-phenanthro[9,10-*c*]pyrazol in the 11-position (Fig. 1). 6-Methoxy-2*H*-phenanthro[9,10-*c*]pyrazol-11-ol (**1a**) and 9-methoxy-2*H*-phenanthro[9,10-*c*]pyrazol-6,11-diol (**1b**) were synthesized by photocyclization and dehydration in 1:1 (v/v) EtOH/H_2O, and characterized by IR, ^{1}H NMR and ^{13}C NMR. Fortunately, the single crystal of **1a** was obtained by the slow solvent evaporation technique from 40:1 (v/v) $CHCl_3$/MeOH. The crystal structure of **1a** was determined. Furthermore, the fluorescence properties of **1a** and **1b** were investigated in the base and neutral media.

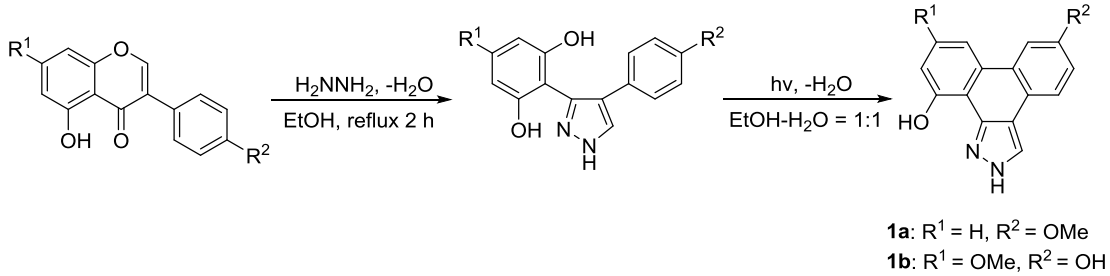

Fig. 1. One-pot synthesis of 2*H*-phenanthro[9,10-*c*]pyrazol-11-ols from isoflavones

2 EXPERIMENTAL

2. 1 Materials and methods

All reagents were commercially available and used without further purification. 4′-Methoxy-5-hydroxyisoflavone and 4′,5,7-trihydroxyisoflavone were purchased from Hebei Guogin Pharmaceutical Company. 4′,5-Dihydroxy-7-methoxyisoflavone was synthesized according to the literature method[20]. Melting points were determined on a X-5 melting point apparatus and uncorrected. The ^{1}H NMR and ^{13}C NMR spectra were recorded on a Bruker AM 400 or Bruker AM 600 instrument in DMSO-d_6. High-resolution mass spectrometry (HRMS) was recorded using electron-spray ionization (ESI) technique and IR spectra were recorded on a Nicollet 170SX FT-IR spectrophotometer using the KBr pellets. All the irradiation experiments were performed in a BL-GHX-V photochemical reactor equipped with a 500 W medium-pressure mercury lamp. Reaction was monitored by thin layer chromatography (TLC) using silica gel 60 GF254 plate. Silica gel (200～300 mesh) was used for column chromatography. The crystal diffraction data were collected on a Bruker Smart-1000 CCD diffractometer.

2. 2 Synthesis and characterization of compounds 1a and 1b

Based on the literature procedure[19], the preparation of 2*H*-phenanthro[9,10-*c*] pyrazol-11-ols was specified in Fig. 1. 3,4-Diaryl-1*H*-pyrazoles were synthesized according to the literature method[20]. Hydrazine hydrate (80%, 5 mmol) was added to an EtOH solution (10 mL) of the appropriate 4′-methoxy-5-hydroxyisoflavone or 4′,5-dihydroxy-7-methoxyisoflavone (1 mmol), and the mixture was refluxed at 80 ℃ until isoflavone was consumed completely indicative by TLC. The mixture was adjusted to pH = 6～7 with a solution of 3 M HCl, and diluted with 40 mL EtOH and 50 mL redistilled water. The solution was contained in 100 mL quartz tubes, deaerated by bubbling argon for 30 min and irradiated with a mediumpressure mercury lamp (500 W) for 10 hours at 20 ℃. The progress of the reaction was monitored by TLC. Then, the solvent was removed under reduced pressure, and the residue was purified by column chromatography on silica gel using chloroform-methanol (40:1) to give the corresponding products **1a** and **1b**, and characterized by ^{1}H NMR, ^{13}C NMR, IR and H RMS.

Data for **1a:** yield 70%, isolated as a pink powder, m.p.: 250.2～251.9 ℃. ^{1}H NMR (600 MHz, DMSO-d_6) δ(ppm) 3.95 (s, 3H), 7.15 (d, J = 7.7 Hz, 1H), 7.28 (d, J = 8.5 Hz, 1H), 7.49 (t, J = 7.9 Hz, 1H),8.09 (s, 1H), 8.23 (t, J = 7.7 Hz, 2H), 8.48 (s, 1H), 10.95 (s, 1H), 13.15 (s, 1H); ^{13}C NMR (150 MHz, DMSO-d_6) δ(ppm) 55.3, 106.5, 111.3, 111.9, 114.8, 115.9, 116.7, 120.8, 124.9, 127.5, 128.1, 130.9, 132.0, 133.0, 153.5, 156.9. IR (KBr) v (cm^{-1}) 3468 (w, N–H), 3181 (b, O–H), 3114, 2931, 2567, 1589, 1471, 1419 (s, benzene skeleton C=C), 1359 (w, C–H), 1253, 1211, 1164, 1066, 952, 844, 800, 692, 651. H RMS (ESI) calcd. for $C_{16}H_{12}N_2O_2$ $[M+H]^+$ 265.0977, found 265.0968.

Data for **1b:** yield 57%, isolated as a pink powder, m.p. 336.5～338.3 ℃. ^{1}H NMR (600 MHz, DMSO-d_6) δ(ppm) 3.93 (s, 3H), 6.75 (s, 1H),7.14 (d, J = 8.0 Hz, 1H), 7.47 (s, 1H), 7.91 (s, 1H), 8.10 (d, J = 8.0 Hz, 1H), 8.38 (s, 1H), 9.60 (s, 1H), 11.01 (s, 1H), 12.95 (s, 1H); ^{13}C NMR (150 MHz, DMSO-d_6) δ(ppm) 55.2, 97.1, 100.5, 106.5, 108.7, 114.9, 117.3, 120.1, 124.8, 128.1, 131.7, 133.0, 142.9, 154.7, 155.1, 158.7. IR (KBr)v (cm^{-1}) 3466 (w, N–H), 3167 (b, O–H), 3109, 2956, 2567, 1591, 1479, 1423 (s, benzene skeleton C=C), 1354 (w, C–H), 1213, 1161, 1068, 956, 800, 656. H RMS (ESI) calcd. for $C_{16}H_{12}N_2O_3$ $[M+H]^+$ 281.0926, found 281.0928.

2. 3 X-ray structure determination

The black prism crystal of compound **1a** with approximate sizes of 0.35mm ×0.29mm ×0.12mm suitable for X-ray diffraction analysis was obtained from the system of $CHCl_3$/MeOH (v/v = 40:1) by slow evaporation at room temperature. The data were collected on a Bruker Smart-1000 CCD diffractometer

equipped with graphite-monochromated Mo*Ka* radiation (λ = 0.71073 Å) by using a ψ-ω scan mode in the range of 2.32<θ<25.09 ° at 296(2) K. A total of 5442 reflections were collected and 2002 were independent (R_{int} = 0.0225), of which 1674 were observed with $I > 2\sigma(I)$ and used in the succeeding refinements. All non-hydrogen atoms were refined anisotropically. All hydrogen atoms were added at the calculated positions and refined using a riding model. The structure was solved by direct methods and refined on F^2 by full-matrix least-squares with SHELX-97 program[22]. The final refinement converged to R = 0.0646 and wR = 0.1487 (w = $1/[\sigma^2(F_o^2) + (0.0921P)^2 + 0.2900P]$, where $P = (F_o^2 + 2F_c^2)/3$), $(\Delta/\sigma)_{max}$ = 0.000, S = 0.986, $\Delta\rho_{(max)}$ = 0.211 and $\Delta\rho_{(min)}$ = –0.214 e/Å^3. Compound **1a** crystallizes in monoclinic, space group $P2_1/c$ with a = 8.8388(17), b = 11.109(2), c = 12.732(2) Å, β = 97.012(3) °, V = 1240.8(4) Å^3, Z = 4, F(000) = 552, D_c = 1.415 g cm^{-3} and μ = 0.095 mm^{-1}.

2. 4 Luminescent properties

The **1a** and **2a** were dissolved in ethanol, being a solution of 1 × 10^{-6} M. The fluorescent spectra of **1a** were measured in different conditions including the base and neutral media with excited slit = 7.5 nm and emission slit = 2.5 nm, and for **1b** the excited slit = 2.5 nm and emission slit = 2.5 nm. Meanwhile, the visual fluorescence was recorded through taking a picture under UV lamp (λ_{ex} = 365 nm).

3 RESULTS AND DISCUSSION

3. 1 Single-crystal structure analysis

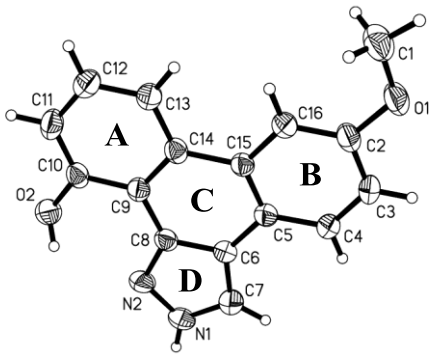

Fig. 2. Molecular structure with atomic numbering for 1a.
Displacement ellipsoids are plotted at the 50% probability level

The molecular structure of **1a** is illustrated in Fig. 2. It consists of four rings, a methoxyl group and a hydroxyl group. The rings include three phenyl rings, A(C(9)～C(14)), B(C(2)～C(5), C(15), C(16)), and C(C(5), C(6), C(8), C(9), C(14), C(15)), and a pyrazole ring D(C(6)～C(8), N(1), N(2)). The atoms of each

ring display an almost coplanar configuration with the mean deviations to their least-squares planes being 0.0014 Å (A and C), 0.0039 Å (B and C) and 0.0028 Å (D and C). Selected bond lengths and bond angles are present in Table 1.

Table 1. Selected Bond Lengths (Å) and Bond Angles (°)

Bond	Dist.	Bond	Dist.	Bond	Dist.
O(2)–C(10)	1.359(3)	N(1)–N(2)	1.346(3)	O(1)–C(2)	1.372(3)
N(1)–C(7)	1.319(3)	O(1)–C(1)	1.412(3)	N(2)–C(8)	1.363(3)
Angle	(°)	Angle	(°)	Angle	(°)
N(2)–C(8)–C(6)	106.8(2)	C(7)–N(1)–N(2)	106.8(2)	C(2)–O(1)–C(1)	118.5(2)
N(1)–N(2)–C(8)	110.7(2)	N(1)–C(7)–C(6)	111.5(2)	O(1)–C(2)–C(16)	124.2(2)
O(2)–C(10)–C(9)	116.1(2)	O(1)–C(2)–C(3)	115.4(2)	N(2)–C(8)–C(9)	130.1(2)

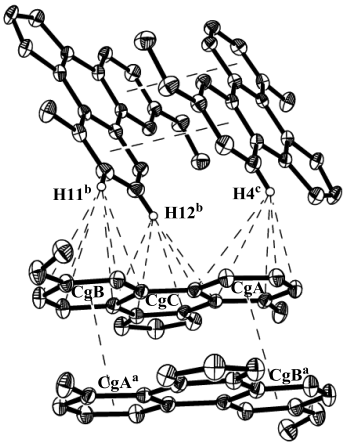

Fig. 3. Part of crystal structure of 1a, showing the C–H ··π and π ··π stacking interactions.
Symmetry codes: (a) –*x*, –*y*, –*z*; (b) –*x*, *y*+1/2, –*z*+1/2; (c) *x*, –*y*+1/2, *z*+1/2

Stacking interaction is a significant research area in supramolecular chemistry and crystal engineering[23-25]. As shown in Fig. 3, there are two kinds of stacking interactions in the crystal structure of **1a**. One is π ··π stacking interaction formed from two neighboring molecules which are arranged in an antiparallel fashion, being rings A and B of a molecular skeleton and rings B and A of another molecular skeleton, with their centriod-centriod distance to be 3.683 Å. The other kind is formed *via* C–H ··π stacking interaction. In the crystal structure of **1a**, three different C–H ··π stacking interactions are displayed, and the distances of H(11)^{b} (symmetry code: (b) –*x*, *y*+1/2, –*z*+1/2) to CgB (CgB is the centroid of ring B), H(12)^{b} (symmetry code: (b) –*x*, *y*+1/2, –*z*+1/2) to CgC (CgC is the centroid of the C) and H(4)^{c} (symmetry code: (c) *x*, –*y*+1/2, *z*+1/2) to CgA (CgA is the centroid of ring A) are 0.3093, 0.2686 and 0.2924 nm, which fall in the normal range of C–H ··π stacking[26]. It shows that the intermolecular interactions, π ··π stacking and C–H ··π interaction exist in the crystal structure of **1a**.

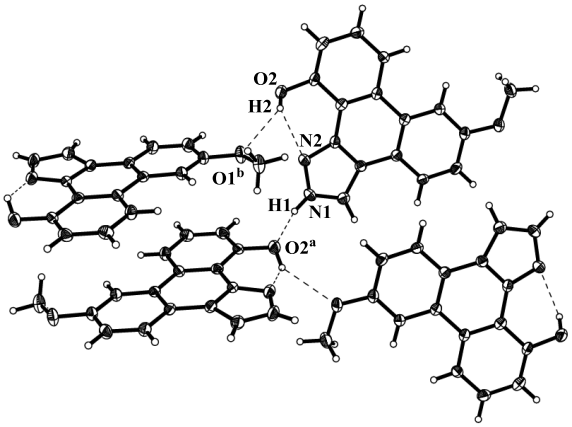

Fig. 4. Sheet of compound 1a formed by intramolecular and intermolecular hydrogen bonds. Symmetry codes: (a) –*x*+1, *y*+1/2, –*z*+1/2; (b) *x*+1, –*y*+1/2, *z*+1/2

As shown in Fig. 4, intramolecular and intermolecular hydrogen bonds exist in **1a**. The intramolecular hydrogen bond O(2)–H(2) ··N(2) (2.729 Å, 116.7 °) is formed between hydroxyl hydrogen atom H(2) and nitrogen atom N(2) of the pyrazole ring D. The molecules are further translated into a chain *via* intermolecular hydrogen bonds. The hydroxyl oxygen atom O(2)^{a} accepts a proton from the other molecule to form intermolecular hydrogen bond N(1)–H(1) ··O(2)^{a} (Symmetry code: (a) –*x*+1, *y*+1/2, –*z*+1/2) with bond length of 2.754 Å and bond angle of 138.8 °, which links molecules of the asymmetric unit together. In addition, hydrogen bond O(2)–H(2) ··O(1)^{b} (symmetry code: (b) *x*+1, –*y*+1/2, *z*+1/2) is observed in adjacent molecules with bond length of 3.205 Å and bond angle of 145.7 °. Details of hydrogen bond lengths and bond angles are also given in Table 2. The $\pi \cdots \pi$, C–H $\cdots \pi$ stacking interaction and hydrogen bonding assemble the crystal structure of **1a** into a three-dimensional network supramolecule.

Table 2. Hydrogen Bond Lengths (Å) and Bond Angles (°)

D–H···A	d(D–H)	d(H···A)	d(D···A)	∠DHA
O(2)–H(2) ··N(2)	0.82	2.261	2.729(3)	117
N(1)–H(1) ··O(2)^{a}	0.86	2.048	2.754(3)	139
O(2)–H(2) ··O(1)^{b}	0.82	2.494	3.205(3)	146

Symmetry codes: (a) –*x*+1, *y*+1/2, –*z*+1/2; (b) *x*+1, –*y*+1/2, *z*+1/2

3. 2 Impact of alkalinity on fluorescence

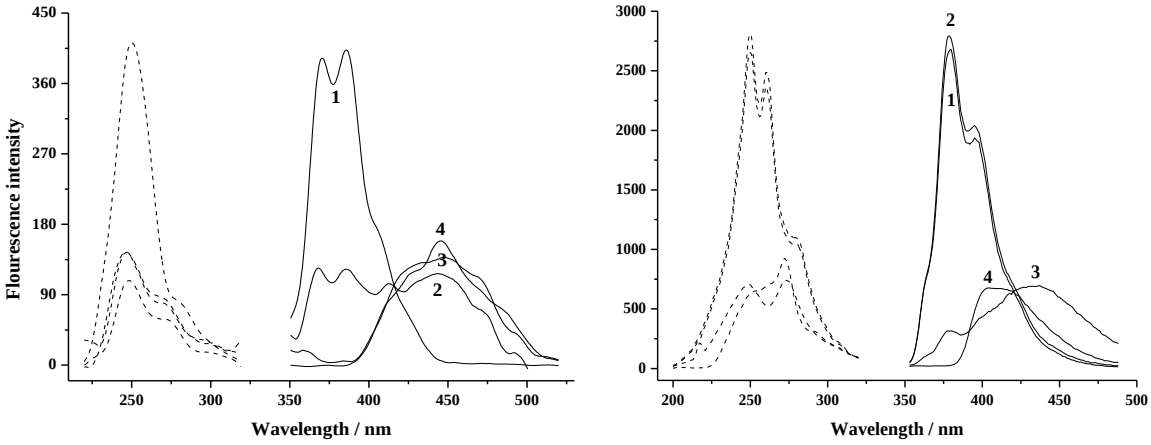

Fig. 5. Excitation spectra (dashed line) and emission spectra (solid line) of 1a and 1b measured in ethanol (solid line 1), 1 × 10^{-5} M NaOH ethanol solution (solid line 2), 1 × 10^{-3} M NaOH ethanol solution (solid line 3) and 1 × 10^{-1} M NaOH ethanol solution (solid line 4); c = 1 × 10^{-6} M

The fluorescence spectra of **1a** and **1b** elucidate their fluorescence behavior that emission maxima has a bathochromic shift with the increase of basicity in different conditions (Fig. 5). Taking **1a** as an example, a very broad fluorescence band is observed at 447 nm by exciting at about 247 nm, and the stokes shift increases to 18114 cm^{-1} in 1×10^{-3} M NaOH ethanol solution. Similarly, the emission spectra of **1b** are also listed in Table 4 and the stokes shift increases to 17277 cm^{-1} in 1×10^{-3} M NaOH ethanol solution (Table 3).

Table 3. Spectroscopic Properties of the Target Products

Compound	Solvent	λ_{ex} (nm)	λ_{em} (nm)	Stokes shift (cm^{-1})
1a	Ethanol	250	385	14025
	Ethanol (1×10^{-5} M NaOH)	247	386	14579
	Ethanol (1×10^{-3} M NaOH)	247	447	18114
	Ethanol (1×10^{-1} M NaOH)	247	445	18014
1b	Ethanol	250	379	13615
	Ethanol (1×10^{-5} M NaOH)	250	378	13545
	Ethanol (1×10^{-3} M NaOH)	249	437	17277
	Ethanol (1×10^{-1} M NaOH)	256	403	14248

In the 1×10^{-5} M NaOH ethanol solution, 11-hydroxyl of **1a** is ionized and the fluorescence spectrum is different from the neutral solution, and 6-hydroxyl of **1b** is ionized and the fluorescence spectrum is similar with neutral solution. Increasing the base ability to 1×10^{-3} M NaOH ethanol solution, 11-hydroxyls of **1a** and **1b** are ionized, and the fluorescence spectra of them show the bathochromic shift and large stokes shift.

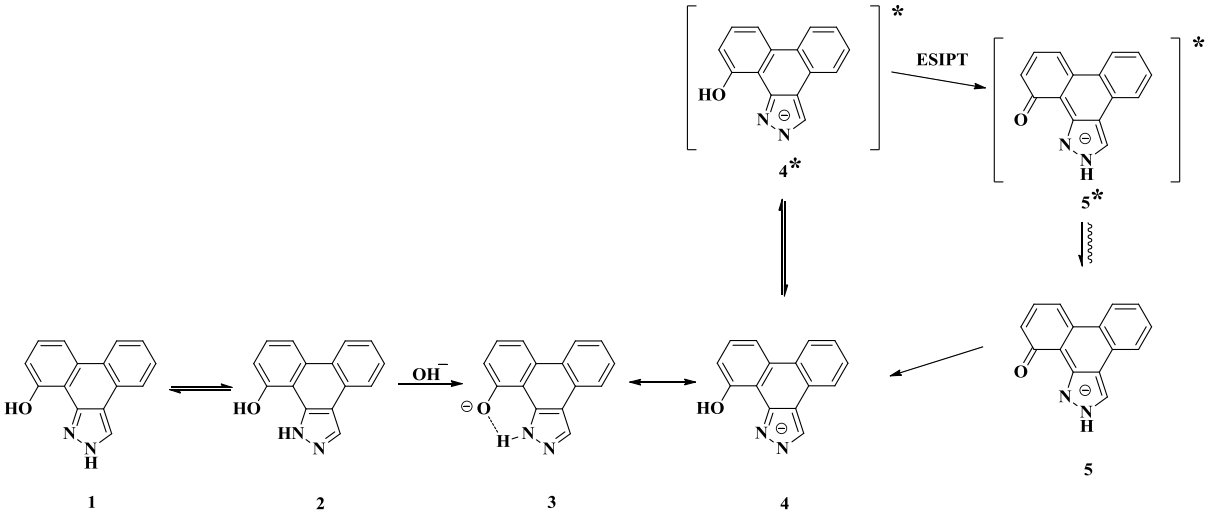

Fig. 6. Excited state intramolecular proton transfer of compounds in alkalinity

The abnormal increase of Stokes shifts and their molecular structures indicate that excited state intramolecular proton transfer (ESIPT) occurred in their molecular skeleton. In neutral solution, **2** was not able to form intramolecular hydrogen bond like N–H ··O because the proton of pyrazole ring is tautomeric. When adding NaOH, tautomer trended to be stable, and **2** existed as the N–H···O tautomer and was beneficial to form anion **3** (Fig. 6). Anion **3** then generated anion keto form **5*** through ESIPT process that phenolic hydroxyl proton transfers to nitrogen in the adjacent pyrazole ring. Then, **5*** emitted yellowish-green light with large Stokes shift when it returned back to the ground state, as shown in Fig. 7. The creation of keto form **5** was followed, which entered a next cycle. Under a UV lamp (λ_{ex} = 365 nm), luminescence of **1a** in the solution of ethanol excited a blue light, and in the solution of base medium ethanol a yellow light appeared (Fig. 7).

Fig. 7. Luminescence of 1a in ethanol (left) and in 1 ×10^{-3} M NaOH ethanol solution (right), excited with a UV lamp (λ_{ex} = 365 nm)

4 CONCLUSION

In summary, 2*H*-phenanthro[9,10-*c*]pyrazol-11-ols **1a** and **1b** were successfully synthesized from isoflavones by two dehydration processes in EtOH. The crystal of **1a** formed a three-dimensional structure by intramolecular interactions (O–H ··N) and intermolecular interactions (N–H ··O, O–H ··O, π ··π, C–H ··π). The fluorescence property studies in the base and neutral media showed that 2*H*-phenanthro[9,10-*c*]pyrazol-11-ols anionic has ESIPT phenomena.

REFERENCES

(1) Hadjoudis, E.; Mavridis, I. M. Photochromism and thermochromism of Schiff bases in the solid state: structural aspects. *Chem. Soc. Rev.* **2004**, 33, 579–588.

(2) Schmidtke, S. J.; Underwood, D. F.; Blank, D. A. Following the solvent directly during ultrafast excited state proton transfer. *J. Am. Chem. Soc.* **2004**, 126, 8620–8621.

(3) Sakai, K. I.; Takahashi, S.; Kobayashi, A.; Akutagawa, T.; Nakamura, T.; Dosen, M.; Kato, M.; Nagashima, U. Excited state intramolecular proton transfer (ESIPT) in six-coordinated zinc(II)-quinoxaline complexes with ligand hydrogen bonds: their fluorescent properties sensitive to axial positions. *Dalton Trans.* **2010**, 39, 1989–1995.

(4) Xu, Y. Q.; Xiao, L. L.; Sun, S. G.; Pei, Z. C.; Pei, Y. X.; Pang, Y. Switchable and selective detection of Zn^{2+} or Cd^{2+} in living cells based on 3′-O-substituted arrangement of benzoxazole-derived fluorescent probes. *Chem. Commun*. **2014**, 50, 7514–7516.

(5) Yang, P.; Zhao, J. Z.; Wu, W. H.; Yu, X. R.; Liu, Y. F. Accessing the long-lived triplet excited states in bodipy-conjugated 2-(2-hydroxyphenyl) benzothiazole/benzoxazoles and applications as organic triplet photosensitizers for photooxidations. *J. Org. Chem.* **2012**, 77, 6166–6178.

(6) Aronoff, M. R.; VanVeller, B.; Raines, R. T. Detection of boronic acids through excited-state intramolecular proton-transfer fluorescence. *Org. Lett.* **2013**, 15, 5382–5385.

(7) Mutai, T.; Sawatani, H.; Shida, T.; Shono, H.; Araki, K. Tuning of excited-state intramolecular proton transfer (ESIPT) fluorescence of imidazo[1,2-*a*]pyridine in rigid matrices by substitution effect. *J. Org. Chem.* **2013**, 78, 2482–2489.

(8) Zhang, Y.; Wang, J. H.; Zheng, W. J.; Chen, T. F.; Tong, Q. X.; Li, D. An ESIPT fluorescent dye based on HBI with high quantum yield and large Stokes shift for selective detection of Cys. *J. Mater. Chem. B.* **2014**, 2, 4159–4166.

(9) Goswami, S.; Manna, A.; Mondal, M.; Sarkar, D. Cascade reaction-based rapid and ratiometric detection of H_2S/S^{2-} in the presence of bio-thiols with live cell imaging: demasking of ESIPT approach. *RSC Adv.* **2014**, 4, 62639–62643.

(10) Elguero, J. *Comprehensive Heterocyclic Chemistry*. Clarendon Press: Oxford **1984**, 167–303.

(11) Elguero, J. *Comprehensive Heterocyclic Chemistry II*. Clarendon Press: Oxford **1996**, 1–75.

(12) Badawey, E.; El-Ashmawey, I. M. Nonsteroidal antiinflammatory agents - Part 1: antiinflammatory, analgesic and antipyretic activity of some new 1-(pyrimidin-2-yl)-3-pyrazolin-5-ones and 2-(pyrimidin-2-yl)-1,2,4,5,6,7-hexahydro-3*H*-indazol-3-ones. *Eur. J. Med. Chem.* **1998**, 33, 349–361.

(13) Wang, H.; Han, H. Y.; Von Hoff, D. D. Identification of an agent selectively targeting DPC4 (deleted in pancreatic cancer locus 4)-deficient pancreatic cancer cells. *Cancer Res.* **2006**, 66, 9722–9730.

(14) Kawanishi, N.; Sugimoto, T.; Shibata, J.; Nakamura, K.; Masutani, K.; Ikuta, M.; Hirai, H. Structure-based drug design of a highly potent CDK1,2,4,6 inhibitor with novel macrocyclic quinoxalin-2-one structure. *Bioorg. Med. Chem. Lett.* **2006**, 16, 5122–5126.

(15) Fletcher, S. R.; Mclver, E.; Lewis, S.; Burkamp, F.; Leach, C.; Mason, G.; Boyce, S.; Morrison, D.; Richards, G.; Sutton, K.; Jones, A. B. The search for novel TRPV1-antagonists: from carboxamides to benzimidazoles and indazolones. *Bioorg. Med. Chem. Lett.* **2006**, 16, 2872–2876.

(16) Chauhan, P. M. S.; Singh, S.; Chatterjee, R. K. Antifilarial profile of substituted pyrazoles: a new class of antifilarial agents. *Indian J. Chem., Sect. B: Org. Chem. Incl. Med. Chem.* **1993**, 32, 858–861.

(17) Xue, W. L.; Warshawsky, D. Metabolic activation of polycyclic and heterocyclic aromatic hydrocarbons and DNA damage: a review. *Toxicol. Appl. Pharmacol.* **2005**, 206, 73–93.

(18) Cai, Y. S.; Guo, Z. Q.; Chen, J. M.; Li, W. L.; Zhong, L. B.; Gao, Y.; Jiang, L.; Chi, L. F.; Tian, H.; Zhu, W. H. Enabling light work in helical self-assembly for dynamic amplification of chirality with photoreversibility. *J. Am. Chem. Soc.* **2016**, 138, 2219–2224.

(19) Wang, Q. Y.; Zhang, Z. T.; Du, Z. C.; Hua, H. L.; Chen, S. S. One-pot synthesis of 2*H*-phenanthro[9,10-*c*]pyrazoles from isoflavones by two dehydration processes. *Green Chem.* **2013**, 15, 1048–1054.

(20) Zhang, Z. T.; Tan, D. J.; Xue, D. A concise one-pot synthesis of 3,4-diaryl-1*H*-pyrazoles from natural isoflavones and hydrazine hydrate. *Helv. Chim. Acta* **2007**, 90, 2096–2018.

(21) Wang, Y. L.; Huang, W.; Chen, S.; Chen, S. Q.; Wang, S. F. Synthesis, structure and tyrosinase inhibition of natural phenols derivatives. *J. Chin. Pharm. Sci.* **2011**, 20, 235–244.

(22) Sheldrick, G. M. *SHELXS-97 and SHELXL-97, Program for Solution and Refinement of Crystal Structure.* University of Göttingen, Germany **1997**.

(23) Ulijn, R. V.; Smith, A. M. Designing peptide based nanomaterials. *Chem. Soc. Rev.* **2008**, 37, 664–675.

(24) Hu, Y. Y.; Xu, W. L.; Li, G. H.; Xu, L.; Song, A. X.; Hao, J. C. Self-assembled peptide nanofibers encapsulated with superfine silver nanoparticles *via* Ag^{+} coordination. *Langmuir.* **2015**, 31, 8599–8605.

(25) Gawade, R. L.; Chakravarty, D. K.; Debgupta, J.; Sangtani, E.; Narwade, S.; Gonnade, R. G.; Puranik, V. G.; Deobagkar, D. D. Comparative study of dG affinity *vs.* DNA methylation modulating properties of side chain derivatives of procainamide: insight into its DNA hypomethylating effect. *RSC Adv.* **2016**, 6, 5350–5358.

(26) Linse, P. Stacked or t-shaped benzene dimer in aqueous solution? A molecular dynamic study. *J. Am. Chem. Soc.* **1992**, 114, 4366–4373.

Crystal Structure and ESIPT Phenomena of Anionic 2*H*-Phenanthro[9,10-*c*]pyrazol-11-ols

LI Chen-Chen(李晨晨)　HE Yun(贺云)　WEI Tao(魏涛)
WANG Tao(王涛)　ZHANG Zun-Ting(张尊听)

2*H*-phenanthro[9,10-*c*]pyrazol-11-ols from isoflavone were synthesized successfully by two dehydration processes, and their anions emit yellowish-green light due to the excited-state intramolecular proton transfer (ESIPT).

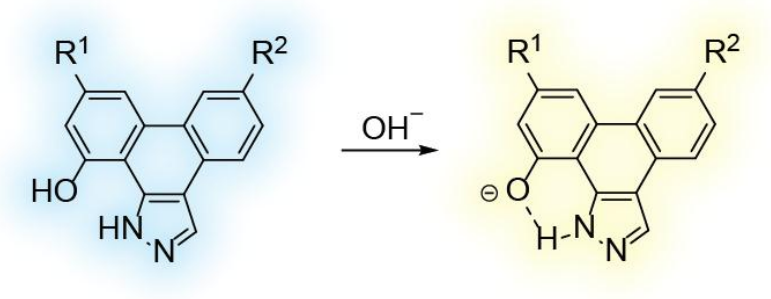

385 nm and 379 nm　　**447 nm and 437 nm**